GS2025-7

Preliminary observations and whole-rock geochemistry of archived drillcore east of Stephens Lake, northeastern Manitoba (parts of NTS 54C, D)

by J. Macdonald

In Brief:

- Archival drillcore east of Stephens Lake was relogged to characterize the stratigraphy of the area
- Preliminary observations and geochemical data indicate these rocks are correlative with the north flank of the Kisseynew domain
- Widespread occurrences of ultramafic rocks may have implications for Ni mineralization

Citation:

Macdonald, J. 2025: Preliminary observations and whole-rock geochemistry of archived drillcore east of Stephens Lake, northeastern Manitoba (parts of NTS 54C, D); *in* Report of Activities 2025, Manitoba Business, Mining, Trade and Job Creation, Manitoba Geological Survey, p. 73–86.

Summary

In June 2025, a field project was initiated to review available geological information on poorly exposed Precambrian rocks east of Stephens Lake in northeastern Manitoba. These rocks are situated north of the Fox River belt and are correlated with the rocks of the Trans-Hudson orogen but have never been the focus of a detailed study to determine their affinity. Industry exploration efforts have targeted these rocks to pursue possible extensions of the Thompson nickel belt and to investigate source rocks for diamondiferous kimberlite indicators in glacial till, which makes assessing their affinity essential to understanding their mineral potential. Thirteen archival drillholes within this area were selected for relogging in the current work. Preliminary findings identify two broad geographic distributions of lithologies: southern holes contain variably migmatized graphitic greywacke and talc-rich ultramafic rocks that locally display a spinifex-like texture, whereas northern holes intersected variably hematized, mafic to ultramafic intrusive rocks, as well as a sequence of felsic to intermediate volcanic rocks and banded iron formation. Geochemical similarities between the metasedimentary rocks in the southern drillholes and those of the northern flank of the Kisseynew domain support a correlation between the two metasedimentary packages; moreover, volcanic arc and mafic to ultramafic intrusive rocks to the north may correlate with the Lynn Lake domain. Fifty samples were collected and will be variably submitted for petrographic thin-section preparation, whole-rock geochemistry, uranium-lead geochronology and samarium-neodymium isotopic analysis to aid in lithotectonic correlations.

Introduction

Little is known of the Precambrian geology north of the Superior province in the Hudson Bay Low-land of northeastern Manitoba. Rock exposures are sparse and Phanerozoic sedimentary rocks overlie much of the Precambrian bedrock. The rocks are interpreted to be correlative with rocks of the northern flank of the Kisseynew domain (KD; Haugh and Elphick, 1968; Corkery, 1985) but are isolated from the KD by an area of poor bedrock exposures and mixed Archean and Paleoproterozoic isotopic signatures that may mark a collisional zone between the Archean Superior craton and the Paleoproterozoic Churchill province (Figure GS2025-7-1; Hartlaub et al., 2005; Böhm et al., 2019). Bedrock mapping, whole-rock geochemistry and samarium-neodymium (Sm-Nd) isotopic data indicate that the rocks of the principal KD extend as far northeast as Rock Lake (Zwanzig and Böhm, 2004). To the northwest, the Owl River shear zone separates the mixed collisional zone from metasedimentary rocks of Archean provenance on Campbell Lake (Hartlaub et al., 2005). The Sm-Nd isotopic characteristics of metasedimentary rocks at Stephens Lake and north of the Fox River belt, referred to in this report as the Stephens Lake assemblage (SLA; Figure GS2025-7-1), indicate a Paleoproterozoic provenance (Rinne, 2018; Böhm et al., 2019).

Bedrock mapping north of the Superior province was conducted primarily at Stephens Lake and the Nelson River prior to hydroelectric dam development in 1971 (Figure GS2025-7-1; Haugh and Elphick, 1968; Frohlinger, 1974; Corkery, 1985), and bedrock exposures are now minimal. Exploratory drill-holes east of Stephens Lake targeted electromagnetic anomalies within these rocks (Figure GS2025-7-1; Assessment Files 74249, 74410, 74005, 74154, 74259, 91728 and 94676; Manitoba Economic Development, Investment, Trade and Natural Resources, Winnipeg) and intersected a diverse suite of rock types that are not commonly observed in the KD or at Stephens Lake. As the lack of bedrock exposures precludes a field mapping program, the current project involves two components:

targeted sampling of the rare shoreline outcroppings of bedrock at Stephens Lake for whole-rock
 Sm-Nd and detrital uranium-lead (U-Pb) zircon analysis to assess provenance and depositional age



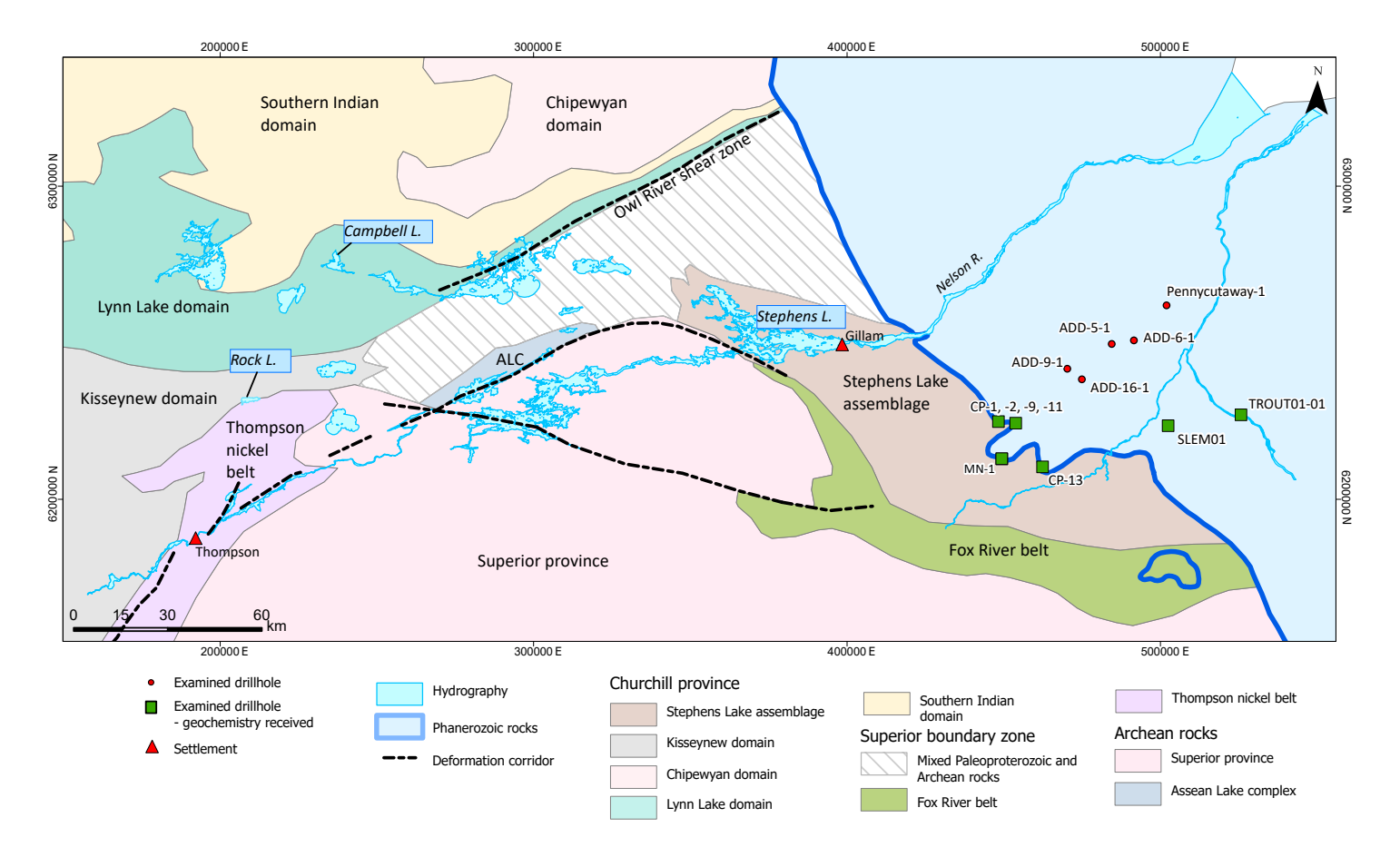


Figure GS2025-7-1: Drillholes of the study area overlain on a simplified lithotectonic map of the Trans-Hudson oragen in east-central Manitoba (after Manitoba Geological Survey, 2024 and Hartlaub et al., 2005). Co-ordinates are in UTM zone 14, NAD83. Abbreviations: ACL, Assean Lake complex; L., lake.

relogging and sampling of selected industry drillholes collared east of Stephens Lake to draw potential correlations with regional lithotectonic packages

Only preliminary findings associated with relogging of the industry drillcore are presented in this report, as the Stephens Lake bedrock-sampling component could not be carried out due to road closures and hazardous conditions associated with wild-fires this past summer.

Regional setting

During the Trans-Hudson orogeny (THO), a series of volcanic arcs and associated sedimentary basins belonging to Churchill province were accreted onto the southern margin of the Archean Hearne craton (ca. 1890 to 1830 Ma; Corrigan et al., 2009). The KD consists of synorogenic turbidites and continental sandstones deposited in a back-arc, intra-arc or fore-arc setting (Zwanzig, 1990; Ansdell et al., 1995; Zwanzig and Bailes, 2010) between 1890 and 1830 Ma (Machado et al., 1999; Lawley et al., 2020). The Burntwood group comprises the majority of the central KD and consists of migmatites and biotite gneisses that contain garnet, sillimanite and cordierite porphyroblasts and minor graphite (Zwanzig, 1990). High-grade metamorphism and intense deformation have made stratigraphic correlations within the Burn-

twood rocks unrecognizable (Zwanzig, 1990); however, a distinct layered amphibolite unit sits at the top of the Burntwood group and is locally associated with calcsilicate rock, iron-rich rock, ultramafic rock, impure marble and chert (Zwanzig, 1990), which are collectively referred to as the Granville complex (Murphy and Zwanzig, 2021). The Granville complex is thought to be in thrust contact with the top of the Burntwood group and to represent the ocean floor onto which the Burntwood group turbidites were deposited (Murphy and Zwanzig, 2021).

The continentally derived Sickle group stratigraphically overlies the Burntwood group on the northern flank of the KD at a contact that can be conformable or structural (Zwanzig, 1990; Ansdell et al., 1995). The Sickle group comprises migmatitic quartz-rich gneisses that commonly contain magnetite and potassium feldspar, and are thought to be derived from lithic sandstone, calcareous sandstone, arkose, conglomerate and argillaceous siltstone (Zwanzig, 1990). Abundant granitoid clasts (Stauffer, 1990) and ca. 1880 to 1833 Ma detrital zircons (Ansdell, 1993; David et al., 1996; Lawley et al., 2020) in the detritus indicate a proximal provenance from the bounding arc terranes and a maximum depositional age of ca. 1833 Ma (Murphy and Zwanzig, 2021).

At ca. 1830–1800 Ma, the northwestern margin of the Superior craton collided with the accreted terranes of the southern Churchill province (Corrigan et al., 2009). Peak metamorphic conditions in the KD reached upper-amphibolite— to granulite—facies (750 \pm 50 °C and 5.5 \pm 1 kbar; Gordon, 1989), caused widespread partial melting and were reached by ca. 1815 Ma (Gordon et al., 1990; Growdon, 2010). Mylonite zones and brittle faults offset the peak metamorphic isograds and postdate the period of folding and anatexis (Zwanzig, 1990). Felsic to mafic calcalkalic magmatism in the central KD occurred from ca. 1840 to 1800 Ma (Bickford et al., 1990; Gordon et al., 1990).

Drillcore descriptions

Approximately 1200 m of drillcore from 13 drillholes collared east of Stephens Lake were selected for relogging (Figure GS2025-7-1). All drillcore examined in the current work is archived at the core storage facilities of the Manitoba Geological Survey and the collar details are provided in the accompanying Data Repository Item DRI2025024 (Macdonald and Janssens, 2025)¹. The examined drillholes were selected to maximize the number of different lithologies described and ensure the widest geographic distribution. Many of the drillholes (8 of 13) returned short intersections (<70 m) of one Precambrian rock type that do not allow for the characterization of genetic relationships between the rock types. Thus, correlations between individual drillholes are difficult. All rocks described here have been metamorphosed; however, the 'meta' prefix has been omitted for clarity.

Peridotite

Pervasively talc- and serpentine-altered rocks were intersected in three drillholes: CP-2, SLEM01 and TROUT01-01. These rocks are light green to grey and display two textural varieties: 1) coarse-grained domains of spinifex-like crystals completely replaced by variable amounts of serpentine, chlorite, actinolite and talc, and commonly associated with fine- to medium-grained magnetite disseminations (Figure GS2025-7-2a); and 2) massive aphanitic intervals that are talc rich and that host up to 10% fine-to medium-grained disseminated magnetite.

The pseudomorphous, spinifex-textured crystals typically lack a preferred orientation but are weakly aligned in one interval (~2.5 m). One ~60 cm interval contains medium- to coarsegrained orthocumulate olivines that are partially to completely serpentinized and set in a talc matrix. Magnetite-rich veins are locally abundant, have jagged, nonplanar margins and crosscut the aphanitic, talc-rich host at a variety of angles. A zone of massive pyrrhotite and pyrite was reported in drillhole TROUT01-01 during the initial drillcore logging (290.5–291.2 m; Assessment File 74249) but the drillcore containing this interval was not available for study during the current work.

Ultramafic rocks containing relict or pseudomorphous olivine and pyroxene are the dominant rock types in drillholes ADD-5-1, ADD-16-1 and ADD-9-1; however, intense alteration has obscured the primary mineralogy. Geochemistry and petrography may assist in differentiating the rocks described in this paragraph. These rocks are dark grey to light green or brick-red, medium to coarse grained and lack a pervasive foliation. Olivine (10-90% locally) is variably altered and has been partially to completely replaced by serpentine, chlorite or hematite. The presence of gradational variations in the abundance of the replaced crystals suggests cumulus crystallization of olivine (Figure GS2025-7-2b). Pseudomorphous, euhedral pyroxene (<1.2 cm) comprises 5–25% of the groundmass and has been strongly chlorite altered. Biotite is locally a major mineralogical component of the groundmass (up to 40%) and occurs as fine-grained crystals in a chlorite-rich groundmass, with local variations in the abundance of serpentine and talc. Magnetite is present throughout the replaced olivine crystals and altered groundmass as fine-grained disseminations (<10%) and locally infills a breccia as coarse, elongate crystals nucleated on the heterolithic fragments. Carbonate minerals (5–15%) occur as round aggregates of crystals that are pink in the cores. The matrix has locally been strongly hematite altered and coarse-grained (<3 cm wide), beige amphibole porphyroblasts (Fe-anthophylite?) appear to overgrow the hematized groundmass (Figure GS2025-7-2c). Serpentine-carbonate veins (<5-50 mm) hosting disseminated magnetite and crosscutting the altered rock are ubiquitous, and locally form a stockwork comprising up to 25% of the rock.

Anorthosite

The one locality in which this rock is observed in drillhole ADD-9-1 is within cumulate-textured peridotite. It is white to beige, very coarse grained and contains ~85–90% randomly oriented, beige plagioclase crystals (up to 3.5 cm wide; Figure GS2025-7-2d). Pseudomorphs consisting of hornblende and biotite comprise the remainder of the rock and developed after a medium-grained, subhedral primary phase. The upper contact of this rock is marked by a selvage of talc and serpentine ~25 cm across and wide fractures (>5 mm) that crosscut the rock are infilled with the same mineral assemblage. Abundant narrow fractures (<5 mm) are infilled with a soft, aphanitic mineral, translucent in appearance, and associated with a halo of brickred hematite alteration 2–5 mm wide (Figure GS2025-7-2d).

Ultramafic schist

Drillhole SLEM01 intersected a ~8 m interval of texturally variable serpentine- and chlorite-rich rock immediately below the Paleozoic unconformity. Regolith is developed near the top of the interval and the rock is poorly preserved in the drillcore.

¹ MGS Data Repository Item DRI2025024, containing the data or other information sources used to compile this report, is available online to download free of charge at https://manitoba.ca/iem/info/library/downloads/index.html, or on request from minesinfo@gov.mb.ca, or by contacting the Resource Centre, Manitoba Business, Mining, Trade and Job Creation, 360-1395 Ellice Avenue, Winnipeg, Manitoba R3G 3P2, Canada.



Figure GS2025-7-2: Drillcore photographs of mafic to ultramafic rocks east of Stephens Lake; all drillcore is NQ^{TM} size (diameter = 4.76 cm): a) spinifex-like pseudomorphs in ultramafic rock (drillhole TROUT01-01, 213.8 m); b) selectively hematite-replaced cumulus olivine in altered peridotite (drillhole ADD-9-1, 113.55 m); c) pervasively hematite-altered ultramafic rock, with beige porphyroblasts overgrowing hematized groundmass (arrows; drillhole ADD-16-1, 94.8 m); d) hematite-altered peridotite (top row), and fractured and altered anorthosite (bottom row; drillhole ADD-9-1, 134.7 m); e) pegmatitic gabbro (top two rows) and diorite (bottom row; drillhole ADD-6-1, 130 m); f) basalt, with coarse-grained pyroxene (centre row) and irregular carbonate vein (bottom row; drillhole SLEM01, 185.5 m).

The ultramafic schist is fine to medium grained and typically has a weak planar fabric defined by aligned chlorite, talc and lesser biotite. Serpentine is abundant along fracture planes and, at the top of the lithology, these bands are aligned subparallel in an anastomosing network.

Gabbro to pyroxenite

Pegmatitic gabbro is the dominant lithology in drillhole ADD-6-1 (Figure GS2025-7-2e). It is mottled black and white and lacks a foliation in hand sample. Diorite and granitic pegmatite dikes sharply crosscut it. Domains of differing grain size grade into one another over intervals ~2–4 m long, although the mineralogy of the different domains is similar. Subhedral to euhedral hornblende (80–85%) is randomly oriented in a matrix of plagioclase (~10–20%). Light brown, well-cleaved titanite crystals are locally observed in the pegmatitic portions and minor amounts of a finegrained, bright green to yellow mineral (epidote?) are also locally observed along cleavage planes in hornblende or along grain boundaries. Chalcopyrite and pyrite are disseminated in trace amounts as fine-grained blebs. The rock has strong magnetic properties locally, and plagioclase crystals are weakly hematized.

Mafic intrusive rocks are present in three drillholes: SLEM01, CP-1 and ADD-9-1. These dark green to grey, medium-grained rocks are composed primarily of dark green amphibole (60–90%), light green pyroxene (10–30%) and interstitial chlorite, which are aligned to define a subtle, continuous foliation. Pyroxene phenocrysts up to 2.5 cm long are locally present and aligned with the foliation (Figure GS2025-7-2f). Fine-grained, interstitial plagioclase, up to 10% locally, occurs in the dark green amphibole groundmass. Sharp contacts are not observed between these rocks and their fine-grained mafic host, and it may be that they represent coarsely recrystallized basalt.

Basalt

Mafic volcanic rocks were intersected in drillhole SLEM01, where they are in contact with semipelitic greywacke, and in drillhole Pennycutaway-1, where they are in sheared contact with quartz porphyry and conformable contact with banded iron formation. These fine-grained rocks are dark green to grey and have a continuous foliation defined by the alignment of amphibole, plagioclase and, locally, pyroxene and chlorite. Garnet is locally present as medium-grained, equant crystals (up to 10%) in a biotite-altered groundmass. Primary features were not identified in the drillcore; however irregularly shaped carbonate veins with biotite- and diopside-bearing selvages may represent altered pillow selvages (Figure GS2025-7-2f). Fine-grained disseminations and millimetre-scale stringers of pyrrhotite are common.

Felsic to intermediate volcanic rocks

Felsic volcanic rocks that vary from light grey to blue are the dominant lithology in drillhole Pennycutaway-1 (Figure GS2025-7-3a-d). The rocks consist of a quartz- and plagioclase-rich

groundmass hosting various proportions of lenticular to amoeboid lithic fragments (<5-20%; 5-30 mm) and plagioclase (2-15%; 2-5 mm), quartz (1-15%, 1-10 mm) and/or dark green amphibole (1-10%) phenocrysts (Figure GS2025-7-3a, b). Sericite-rich bands (2-5%, 1-4 cm wide) and amphibole-rich bands (1-5%, 1-8 cm wide) are present throughout. Garnet occurs as fine- to medium-grained crystals in amphibole-rich bands and as fine-grained aggregates of crystals in the quartzofeldspathic groundmass. Medium-grained euhedral magnetite (<8 mm) is locally hosted in the groundmass and trace amounts of pyrrhotite occur as fine-grained stringers that parallel the foliation. Arsenopyrite is locally associated with quartz veining or occurs as finegrained disseminations in the groundmass (2–3% over 30 cm). Zones of alteration (<4 m wide) grade into the unaltered rock and contain biotite (15%), chlorite (<10%), andalusite (<10%) and garnet (1-8%); the presence of andalusite porphyroblasts (up to 15%) is also noted in a 1.6 m interval lacking a pervasively altered groundmass and in which they overgrow select compositional bands. Four varieties of lithic fragments (lapilli?) are observed:

- an aphanitic to fine-grained light grey rock that contains 15%
 K-feldspar and 5–15% dark green amphibole
- light green fragments with cores hosting 10% fine-grained, dark grey quartz and fine-grained epidote with aphanitic white rims
- a light pink and aphanitic rock with 10% fine-grained, dark green amphibole
- rare, round fragments (0.5–1.5 cm wide) that are dark grey and quartz rich, host fine-grained green inclusions and lack a reaction rim

A foliation is defined by the elongation of quartz phenocrysts, plagioclase phenocrysts and/or lithic fragments, and the alignment of amphibole and plagioclase in the groundmass. Variations in relative abundances of fragments and mineral constituents define compositional bands that are parallel to the foliation. Graded beds (5–15 cm wide) are locally present and have tops oriented downhole, as indicated by gradational increases in the abundance of biotite and amphibole. Lithic fragments are rotated in the foliation and have recrystallized tails. A sericiterich mylonitic zone overprints the continuous foliation over a ~60 cm interval and marks a contact with basalt.

Quartz porphyry

This porphyritic unit is in sharp contact with amphibolite and banded iron formation in drillhole Pennycutaway-1 (Figure GS2025-7-3b, d). It comprises a dark grey to beige aphanitic and siliceous groundmass hosting anastomosing bands of finegrained sericite (10–15%), dark green fine- to medium-grained amphibole (5–15%), medium-grained biotite (5–10%) and blue grey 'quartz eyes' (1–12%). These minerals are aligned to define a foliation that wraps the quartz eyes. Garnet occurs as fine-grained pinpricks in the amphibole-rich domains and as medium-grained (3–6 mm) crystals that are associated with quartz phenocrysts

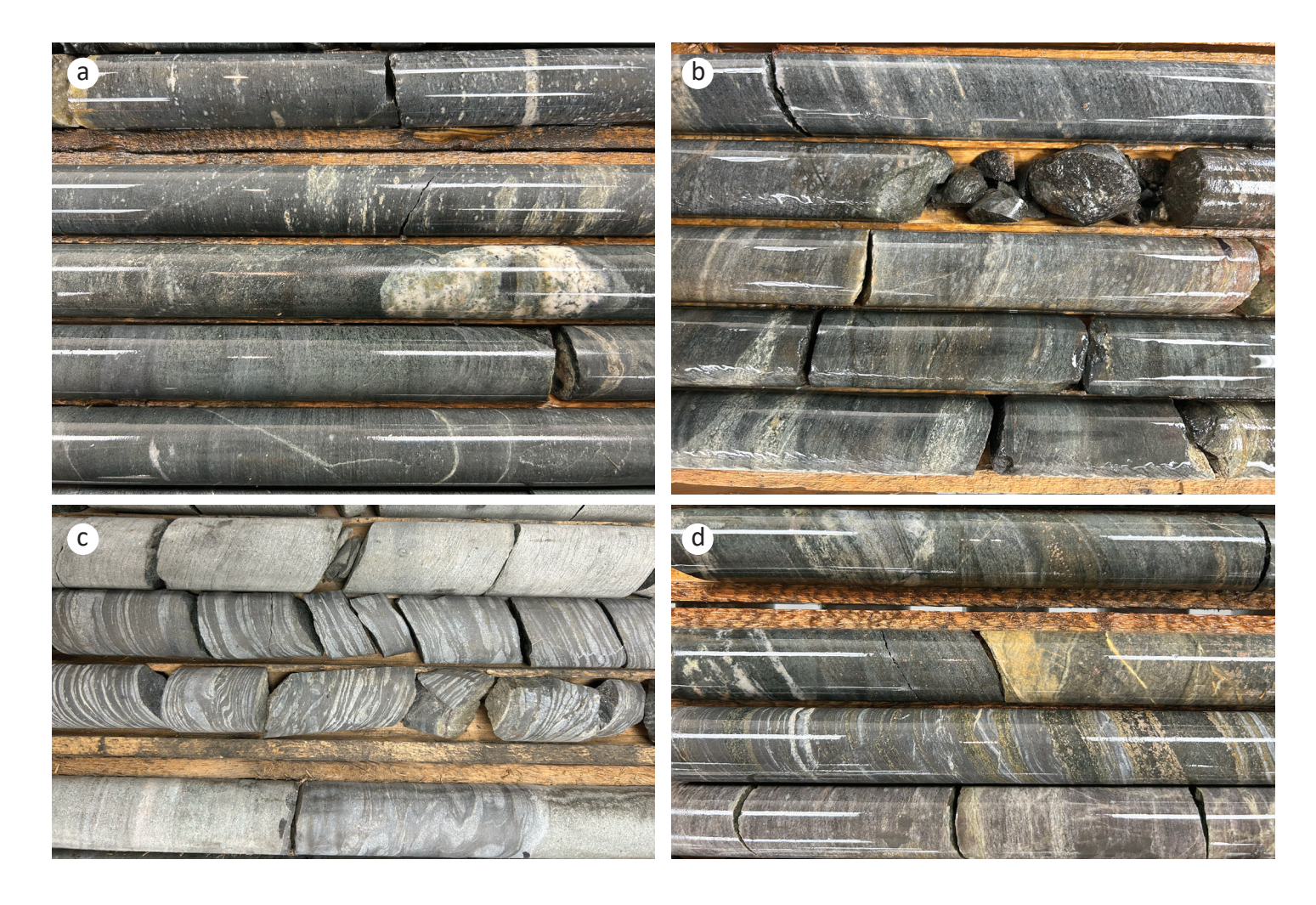


Figure GS2025-7-3: Drillcore photographs of felsic to intermediate volcanic rocks east of Stephens Lake; all drillcore is AQ^{TM} size (diameter = 2.70 cm):

a) felsic to intermediate volcanic rock (drillhole Pennycutaway-1, 404.6 m); b) felsic to intermediate volcanic rock (top two rows), quartz porphyry (middle row) and basalt (bottom rows; Pennycutaway-1, 236.5 m); c) felsic to intermediate volcanic rock (top row) and banded iron formation (bottom three rows; Pennycutaway-1, 352.3 m); d) intercalated amphibolite (top two rows), banded iron formation and quartz porphyry (bottom two rows, respectively; Pennycutaway-1, 370.6 m).

and overgrow the foliation. Cummingtonite is locally present as light brown to yellow, fine-grained equant crystals that selectively overgrow select beds with amphibole, garnet and biotite. Pyrrhotite (1–5%) occurs primarily as fine-grained stringers or in a net-texture, where it is most abundant.

Rhyolite

Light grey, aphanitic felsic dikes crosscut altered peridotite in drillhole ADD-16-1. The rock contains 1–4% fine-grained plagioclase crystals randomly oriented in an aphanitic siliceous groundmass. Fine-grained actinolite (~2%) is present throughout and hematite alteration permeates the matrix. A fragmental texture is locally present, in which ovoid fragments of this rock are aligned in an anastomosing matrix of foliated, medium-grained biotite.

Semipelitic greywacke

A muscovite-biotite schist was intersected in MN-1 and SLEM01 (Figure GS2025-7-4a) and interpreted to represent a semipelitic greywacke. These rocks are light blue to grey and have a prominent schistosity defined by layers of medium-grained muscovite (2–10%), biotite (2–10%) and local sillimanite knots (<1%–8%) in a matrix of quartz and plagioclase. Primary textures are not common, but variations in the relative proportions of the above minerals likely represent bedding. Garnet is observed in a few locations as medium-grained euhedral crystals set in biotiterich folia. Where sillimanite is present, biotite is more abundant than muscovite. Pyrrhotite is present throughout the rock as millimetre-scale laminations along the schistosity planes. There are broad changes in the orientation of the schistosity over 1–10 m intervals and crenulations in the schistosity are commonly present.

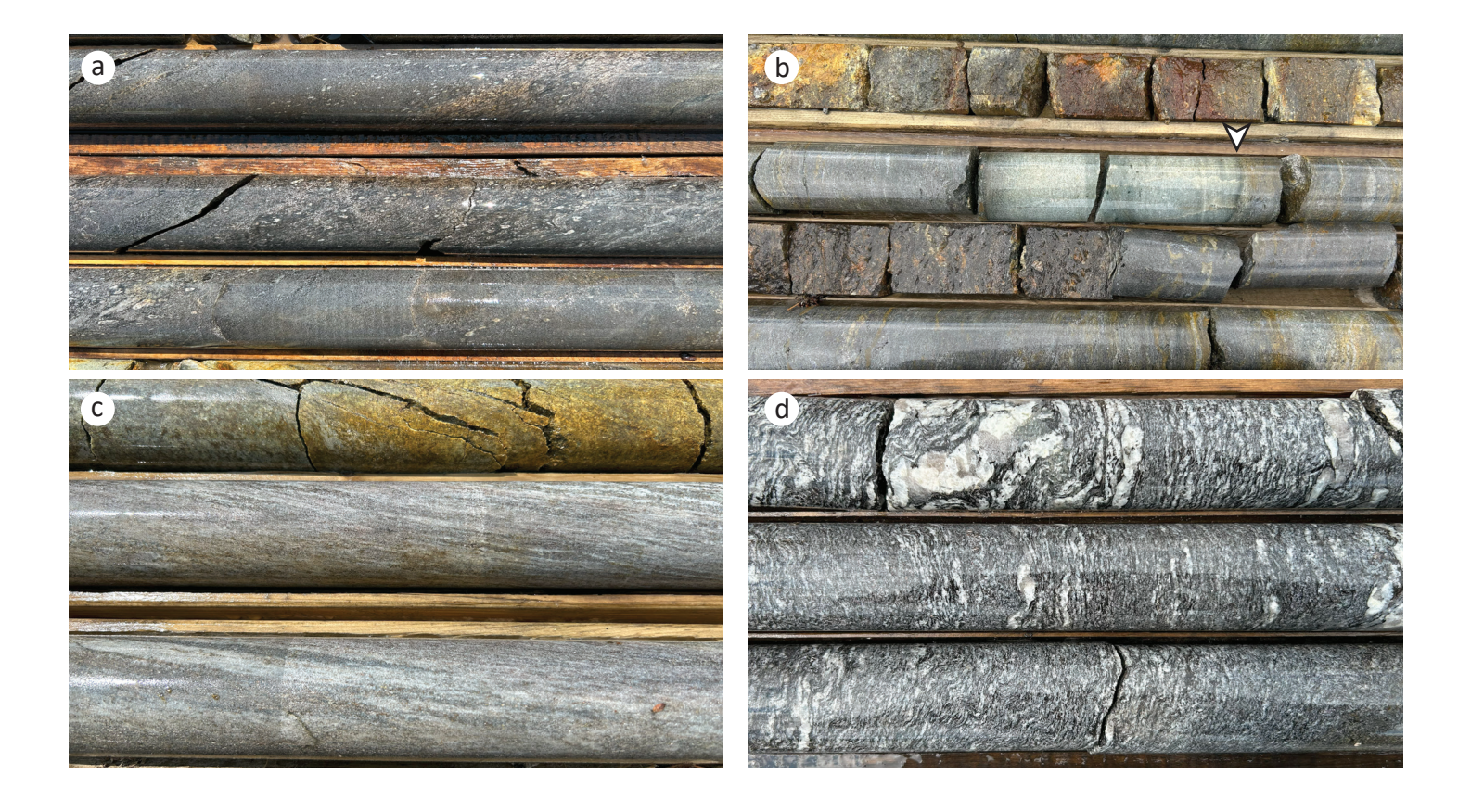


Figure GS2025-7-4: Drillcore photographs of metasedimentary rocks east of Stephens Lake; all drillcore is NQ^{TM} size (diameter = 4.76 cm): **a)** semipelitic greywacke, with beds of differing composition (drillhole SLEM01, 252.3 m); **b)** sulphidic and graphitic mudstone, with gradational contact on siliceous (chert?) layer (arrow; drillhole MN-1, 108.0 m); **c)** strained calcsilicate rock (drillhole MN-1, 214.0 m); **d)** migmatitic biotite-sillimanite gneiss (drillhole MN-1, 256.3 m).

Feldspathic wacke

This texturally and mineralogically homogeneous rock was encountered in drillhole CP-9 over a 66 m drilled interval. It is light grey to blue, medium grained and has a continuous foliation defined by the alignment of quartz, plagioclase and biotite. Medium-grained quartz and plagioclase are present in roughly equal amounts, and fine- to medium-grained biotite (5–10%) occurs as aggregate clusters aligned with the foliation. Muscovite intergrown with biotite is locally present. Fracture networks impart a brecciated texture over intervals of ~1–2 m and are associated with weak pervasive silicification.

Mudstone

Sulphide- and graphite-bearing mudstone was encountered in drillhole MN-1 (Figure GS2025-7-4b). This rock is black, aphanitic to fine grained and is in gradational contact with the muscovite-biotite-quartz schist that is marked by a decrease in the abundance of quartz and feldspar and an increase in the

abundance of biotite, graphite and sulphide minerals. The two rock types are intercalated in segments of 1–3 m over an interval ~10 m long. The groundmass of the rock is composed largely of biotite, which is aligned to define a foliation that is parallel to the overall trend of abundant discontinuous and chaotically folded layers (<1.5 cm wide) of pyrite, pyrrhotite and local chalcopyrite. Graphite occurs as fine-grained aligned flakes, wispy layers and rarely in massive to net-textured intergrowths with pyrrhotite. Pyrrhotite locally forms a net texture around fragments of the biotite matrix. Narrow (<20 cm), siliceous (cherty?) horizons contain up to 5% muscovite and are separated from the graphitic mudstone by narrow (<4 mm) gradational contacts (Figure GS2025-7-4b).

Calcsilicate rock

This rock is observed in drillhole MN-1 in sharp contact with the semipelitic greywacke. The rock is white to light green, with a banded and mottled texture that varies in orientation and

strain intensity locally. The banding is defined by differences in modal mineralogy and comprises a white, aphanitic and siliceous groundmass with bands of light green diopside (5–20%), discontinuous bands of pyrrhotite (5–8%), disseminated finegrained cubic pyrite (2–3%) and trace amounts of blebby chalcopyrite (<8 mm across). Local patches of calcite (~2–4%) occur in the white matrix. Medium-grained biotite and muscovite form laminations locally, and flakes of bright green chlorite form the foliation in a few instances. Locally, crystals of a fine-grained, subhedral acicular amphibole (3–5%) are randomly oriented. Near the bottom of the drilled interval, the strain intensity increases and the compositional layering is replaced by a ribbon texture (Figure GS2025-7-4c).

Iron formation

Banded iron formation occurs in conformable contact with basalt and felsic to intermediate volcanic rocks in drillhole Pennycutaway-1 (Figure GS2025-7-3c). These rocks contain alternating laminae of aphanitic magnetite and quartz and locally host zones up to 2 m across comprising massive chlorite that hosts disseminations of medium-grained, euhedral magnetite (up to 20 vol. % of the rock) and ovoid domains of quartz set in an anastomosing network of fine- to medium-grained pyrite and pyrrhotite (up to 50 vol. % of the rock). Locally, the anastomosing networks of sulphide minerals host medium-grained euhedral magnetite. Randomly oriented, fine-grained flakes of chlorite can overgrow the magnetite-rich bands, and local patches of sericite and anthophyllite are present. Rootless and intrafolial isoclinal folds in the bands are common and local high-strain zones comprise a network of fine-grained magnetite anastomosing around lenticular domains of quartz. Light yellow, equant cummingtonite overgrows select quartz-rich laminations and gradationally increases in abundance nearing the adjacent magnetite lamina. Narrow intervals of the banded iron formation are intercalated with amphibolite and contain <10% quartz bands. Amphibolerich bands (up to 7 cm wide) are common in these intervals and host fine-grained magnetite, garnet and cummingtonite (Figure GS2025-7-3d).

A texturally and mineralogically heterogeneous unit tentatively interpreted as iron formation was intersected over a ~20 m interval in drillhole MN-1. The strongly magnetic unit is dark grey to brown, hosted in the semipelitic greywacke and contains mineralogical bands overprinted by a weak continuous foliation. Rubbly, hand-split drillcore did not allow for the contact with the host to be observed. The rock contains fine-grained, light green pyroxene (20–30%); medium-grained biotite (10–20%); semimassive to finely disseminated pyrrhotite (5–0%); banded and fine-grained, light red garnet (<1–8%); and trace amounts of a fine-grained, light brown amphibole locally. Conformable bands of blue-grey quartz (1–4 cm wide) can contain massive to nettextured pyrrhotite and medium-grained euhedral crystals of magnetite. Graphite is locally present (2–4%) as isolated flakes with the net-textured pyrrhotite or as semi-massive bands.

Migmatitic biotite-sillimanite gneiss

A migmatitic biotite-sillimanite gneiss was encountered in drillholes MN-1 and CP-13. This rock is light grey and characterized by a strong gneissosity defined by alternating bands of biotite and quartz and plagioclase (Figure GS2025-7-4d). The orientation of the gneissosity broadly changes over metre-scale intervals and parasitic, open to isoclinal folds are common. Quartz in the groundmass (~35%) is medium grained, elongate in the foliation and intergrown with fine-grained plagioclase (~25%). Biotite (10-20%) occurs as medium-grained bands that are aligned to define the foliation of the rock. Muscovite (<5%) is locally present as medium-grained crystals intergrown with biotite and can be euhedral with no preferred orientation, or anhedral and aligned with the gneissosity. Coarse-grained to pegmatitic leucosome comprises 5–20% of the rock as segregations up to 30 cm wide that are concordant with the gneissic fabric and lack an internal foliation. These domains consist of quartz, K-feldspar, plagioclase, and minor biotite and muscovite. Wider pods of leucosome (>1 cm wide) have sharp contacts with a welldeveloped margin of biotite-rich melanosome, whereas narrow pods (<1 cm) have diffuse margins that grade into the gneissosity and lack well-defined melanosome. The abundance of leucosome and biotite varies locally, with intervals up to 8 m long that lack leucosome and contain less biotite (<3%), which may represent primary compositional differences. Narrow mylonitic zones (<2 cm wide) with narrow strain gradients are rarely present, contain muscovite, and crosscut the leucosome and melanosome. One graphitic horizon (~60% graphite over 70 cm) contains concordant bands of pyrrhotite (<5 mm wide) that are set in the fine-grained graphitic matrix and constitute up to 10% of this interval.

Granite

This light grey to pink rock hosted in massive peridotite was intersected in drillhole ADD-5-1. It is fine-grained and has a strong continuous foliation defined by the alignment of K-feld-spar (35–40%), quartz (25–30%), plagioclase (20–25%), biotite (3–4%) and hornblende (3–4%). Quartz ribbons are well developed and a light green aphanitic alteration of the rock matrix is observed over intervals of ~10 cm. The lower contact of the dike is marked by a ~60 cm interval of strongly foliated light beige, soft minerals that are host to elongate amphibolite boudins. The rock is crosscut by numerous inconsistently oriented fractures that are associated with narrow (<1 cm wide) selvages of pervasive hematite alteration.

Granodiorite

Dark-red, medium-grained and massive to weakly foliated granodiorite dikes are hosted as narrow intrusions (5–20 cm wide) and boudins in the altered peridotite of drillhole ADD-5-1. The dikes contain plagioclase (35–50%), quartz (10–35%), dark green amphibole (7–10%) and K-feldspar (5–10%), which are

weakly aligned to define the foliation. Trace amounts of a fine-grained disseminated black, metallic, nonmagnetic mineral are locally present. Alteration haloes of hematite can locally occur immediately adjacent to the granodiorite contacts (~1 cm from the contact) and are in sharp contact with an outer facies of epidote alteration (~5 cm from the contact). Coarse-grained, bladed, brown amphibole is present throughout the alteration halo. The dikes are crosscut by abundant millimetre-scale fractures mantled by a hematite selvage 3–5 mm wide, and in which biotite has crystallized along a central line.

Monzogranite

This rock observed in drillhole CP-11 is not in contact with any other lithology. The rock is light grey to pink and medium grained. The dominant mineralogical components are K-feldspar (40%), quartz (20%), plagioclase (20%), hornblende (5–10%), magnetite (2–8%), biotite (1–4%), garnet (<1%) and chalcopyrite (<1%). Quartz and feldspars do not show any preferred orientation in hand sample, but biotite and hornblende are aligned to define a weak foliation. Magnetite occurs as fine- to mediumgrained disseminations and chalcopyrite is locally present as irregularly shaped blebs <6 mm across. Pegmatitic segregations (<50 cm) have a simple mineralogy of quartz, K-feldspar, plagioclase, muscovite and, locally, biotite; they also have narrow (<3 mm) gradational contacts with the granitoid host.

Diorite to quartz diorite

These rocks are observed in drillholes ADD-5-1, ADD-6-1 and Pennycutaway-1 (Figure GS2025-7-2e). They are light grey and medium grained, with a subtle continuous foliation defined by a weakly aligned groundmass of plagioclase (60–70%), quartz (10%), biotite (5–15%) and hornblende (3–15%), in which equant quartz or aligned plagioclase phenocrysts are locally present. Trace amounts of fine-grained red garnet locally occur along the amphibole grain boundaries.

Tonalite

This light grey to pink rock is observed in drillhole ADD-9-1. It is medium-grained and massive, and contains plagioclase (60%), quartz (30%), dark green amphibole (7%) and biotite (3%). It is crosscut by numerous fractures (~2–6 cm thick) that are infilled with light brown clay minerals. Biotite and amphibole are lightly hematized along grain boundaries. Contact relationships of this unit are not observed, but a narrow rim of brick-red hematite alteration is present within the dike, less than 5 mm from the dike contacts.

Pegmatite

Massive, pink granitic pegmatites (up to 60 cm wide) crosscut the gabbro and altered peridotite in drillholes ADD-5-1 and ADD-6-1 at sharp, planar contacts. The dikes are rich in megacrystic K-feldspar and contain lesser amounts of quartz, plagioclase,

biotite and magnetite. In drillhole CP-9, one such pegmatite crosscuts the feldspathic wacke and hosts a clot of fine- to coarse-grained black tourmaline along its lower contact, which is locally intergrown with an unidentified fine-grained, silvery, mineral of metallic lustre and tabular habit.

Metamorphism

The metamorphic grade of the examined rocks indicates regional amphibolite-facies conditions. In the south, the metamorphic grade is best indicated in the mineral assemblages of the semipelitic greywacke (muscovite-biotite-sillimanite±garnet) and migmatitic biotite-sillimanite gneiss (biotite-sillimanitemelt), which indicate lower-amphibolite and upper-amphibolite—to granulite—facies conditions, respectively (Palin and Dyck, 2021). In the northern drillholes, amphibolite-facies conditions are suggested by the mineral assemblages of pegmatitic gabbro (hornblende-epidote-plagioclase) and banded iron formation (amphibole-garnet-biotite-magnetite). Muscovite-bearing mylonitic zones crosscut the migmatitic biotite-sillimanite gneiss in the south and the felsic to intermediate volcanic rocks in the north and may indicate localized metamorphic retrogression.

Geochemistry

Whole-rock lithogeochemistry results from samples collected in the southern drillholes (CP-1, CP-2, CP-9, CP-11, CP-13, SLEM01, MN-1 and TROUT01-01) are summarized here. A description of the analytical procedures and a full set of the initial geochemical results are available in the accompanying DRI (Macdonald and Janssens, 2025). Geochemistry results for the remainder of the drillholes (ADD series and Pennycutaway-1) are pending. As monzogranite was the only granitoid rock analyzed in the current dataset, discriminatory plots are not included; Nb, Ta, Yb, Y and Rb abundances of this rock indicate volcanic arc affinity (Pearce et al., 1984).

Whole-rock geochemical compositions of the complete dataset are plotted on a Zr/Ti versus Nb/Y volcanic rock discrimination diagram (Figure GS2025-7-5a). Rocks that plot as basaltic in composition are further discriminated by their Ti/V ratios (Figure GS2025-7-5b) and normal mid-ocean—ridge basalt (N-MORB) normalized trace-element profiles (Figure GS025-7-5c). Basalt and pyroxenite in drillhole SLEM01 have Ti/V ratios ranging from 28.9 to 31.4 (Figure GS2025-7-5b) and trace-element abundances indicative of E-MORB affinity (enrichment in Th and Nb and slight enrichment in Zr relative to Ti and Y; Figure GS2025-7-5c), whereas gabbro from CP-1 has characteristics indicative of volcanic arc affinity (Ti/V = 12.7; low trace-element abundances and relative depletions in Nb and Zr relative to Y; Figure GS2026-7-5b, c).

Peridotite samples are not plotted on Figure GS2025-7-5a due to Nb, Y and Zr abundances being below detection limits, but are included with basaltic rocks in the Ti/V and multi-element diagrams due to their high Cr and Ni contents (>2000 ppm Cr and

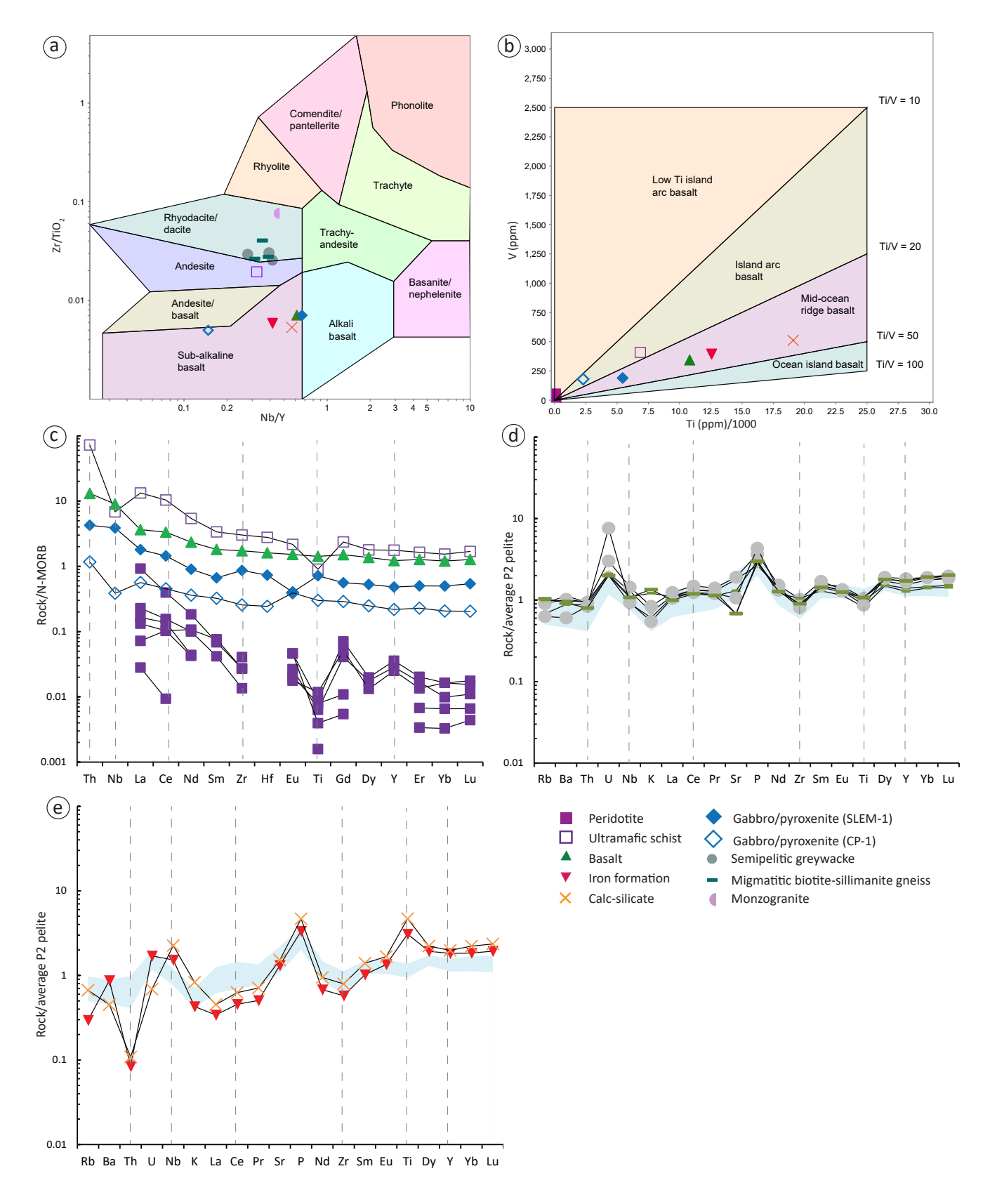


Figure GS2025-7-5: Geochemical plots of whole-rock compositions in drillholes CP-1, CP-2, CP-9, CP-11, CP-13, SLEM01, MN-1 and TROUT01-01; a) Zr/Ti versus Nb/Y volcanic rock classification diagram (after Winchester and Floyd, 1977); b) Ti versus V basalt discrimination diagram (after Shervais, 1982); c) normal mid-ocean-ridge basalt (N-MORB) normalized multi-element plots of mafic to ultramafic rocks (element order after Murphy and Zwanzig, 2021; normalized values from Sun and McDonough, 1989); d, e) average P2 pelite-normalized multi-element plots (after Zwanzig et al., 2007) of semipelitic greywacke and migmatitic biotite-sillimanite, and of calcsilicate and iron formation, respectively, compared with characteristic pattern of Burntwood group metagreywacke-mudstone (light blue field) from Murphy and Zwanzig (2021).

>1000 ppm Ni). Multi-element profiles of peridotite are largely incomplete due to the low trace-element abundances but display negatively sloped profiles with consistent depletions in Ti and Dy relative to Gd and Y (Figure GS-2025-7-5c). The Ti/V ratios range from 0.999 to 11.2, consistent with island-arc basalts; however major-element abundances in the peridotite samples indicate these rocks experienced significant alteration (loss-on-ignition >15%; Macdonald and Janssens, 2025); therefore, a more thorough analysis will be needed for geochemical characterization of the samples.

Murphy and Zwanzig (2021) showed that the metasedimentary rocks in the KD and the Superior boundary zone (Ospwagan, Burntwood and Sickle groups, and Granville complex) can be distinguished by multi-element profiles normalized against the average whole-rock composition of the P2 member of the Ospwagan group, as in Zwanzig et al. (2007; Figure GS2025-7-5d, e). The semipelitic greywacke and migmatitic biotitesillimanite gneiss have parallel trace-element profiles that are characterized by depletions in Zr and Ti, and enrichments in U and P (Figure GS2025-7-5d). The semipelitic greywacke contains comparatively higher U relative to the migmatitic gneiss, which shows slight K enrichment and Sr depletion relative to the semipelitic greywacke in 2 of 3 samples. The calcsilicate and iron formation in drillhole MN-1 have different trace-element characteristics than the host semipelitic greywacke and display slightly positively sloped profiles, with prominent Th, La and Zr depletions and Nb, P and Ti enrichments (Figure GS2025-7-5e). The Zr/Ti and Nb/Y ratios of these two rocks also differ from those of the other metasedimentary lithologies and plot in the basaltic field (Figure GS2025-7-5a), with MORB-type Ti/V ratios (31.8 and 37.4, respectively; Figure GS2025-7-5b). These rocks did not preserve any distinctive primary features, but their geochemical composition suggests that they may have derived from a different provenance, or represent hydrothermally altered and metamorphosed basalts of MORB affinity.

Discussion

Two broad distributions of lithologies are identified in the current project: a southern domain, in which drillholes intersected primarily terrigenous metasedimentary rocks and mafic to ultramafic rocks (drillholes CP-1, CP-2, CP-9, CP-11, CP-13, SLEM01, MN-1 and TROUT01-01); and a northern domain, characterized by mafic to ultramafic intrusive rocks and a felsic to intermediate volcanic sequence intercalated with banded iron formation (drillholes ADD-5-1, ADD-6-1, ADD-9-1, ADD-16-1 and Pennycutaway-1). The lack of field relationships and sparse spacing of the observations limit potential tectonic interpretations; however, correlations may be drawn with the exposed and better studied rocks to the west. It should also be noted that the lithologies are likely not representative of the regions as the examined drillholes selectively targeted conductive and electromagnetic anomalies.

The lithological, metamorphic and trace-element characteristics of the semipelitic greywacke and migmatitic biotite-sillimanite gneiss in the southern drillholes (Stephens Lake assemblage) are similar to those of the Burntwood group (Murphy and Zwanzig, 2021), which comprises the majority of the central KD (Zwanzig, 1990). Furthermore, Nd-model ages of metasedimentary rocks on Stephens Lake and north of the Fox River belt (1.95 and 2.30 Ga, respectively; Rinne, 2018; Böhm et al., 2019) indicate derivation from Paleoproterozoic crust, like the KD. Samples of the semipelitic greywacke and migmatitic biotite-sillimanite gneiss from SLEM01 and MN-1, respectively, were collected for detrital zircon geochronology and should help to further constrain the provenance and timing of deposition in the SLA.

Several rock types described here are similar to those described in the Granville complex, which transects the northern flank of the KD (Murphy and Zwanzig, 2021):

- MORB-type mafic to ultramafic rocks
- mottled, white to brown calculicate rocks containing varying proportions of plagioclase, diopside, calcite and amphibole
- rusty, green to grey-brown iron formation that grades into, or is interlayered with, less sulphidic paragneiss, cherty layers, or mudstone

The multi-element profiles of the basalt, iron formation and calcsilicate rock reported here (Figure GS2025-7-5c, e) are like those of the Granville complex (Murphy and Zwanzig, 2021), further supporting a correlation between the two regions. On Stephens Lake, a layered amphibolite commonly marks the contact between graphitic turbidites and magnetiferous arkoses (inferred Burntwood and Sickle groups, respectively; Corkery, 1985), perhaps representing a continuation of the Granville complex through Stephens Lake as well.

The occurrence of gabbroic and volcanic rocks in the northern domain of the current study area may represent an eastern continuation of the Lynn Lake domain. In western Manitoba, the Lynn Lake domain bounds the northern flank of the KD and represents a series of juvenile oceanic volcanic arcs, associated sedimentary basins and plutons (Gilbert et al., 1980) that are host to numerous different deposit types (orogenic Au; Cu-Zn volcanogenic massive sulphide and magmatic Ni-Cu-Co). The pending geochemistry results from the northern drillholes (ADD series and Pennycutaway-1) will be compared to the well-documented geochemistry of the volcanic (Zwanzig, 1999) and intrusive (Yang, 2025) rocks of the Lynn Lake belt to elucidate any potential correlations.

Economic considerations

Nickel

Drillholes examined in the current work (Assessment Files 74154, 74249, 74410) targeted rocks thought to be extensions of the Thompson nickel belt (TNB); therefore, one of the cur-

rent project goals is to assess similarities between the rocks of the two regions. As Ni-Cu mineralization in the TNB is thought to be associated with the intrusion of ultramafic magmas into the sulphidic horizons in the Ospwagan group (Bleeker, 1990; Zwanzig et al., 2007; Lightfoot et al., 2017), exploration efforts focus largely on the identification of ultramafic rocks or the sulphidic horizons in the metasedimentary hostrocks (e.g., Zwanzig et al., 2007). The metasedimentary rocks in the current work are geochemically different than those of the Ospwagan group, and the available geological evidence does not support a correlation between the studied ultramafic rocks and those of the TNB. However, ultramafic rocks in the northern SLA are now identified over a distance of ~80 km, some of which are in close spatial association with sulphidic sedimentary rocks (i.e., drillhole SLEM01). No instances of ultramafic intrusion into the metasedimentary country rocks were observed but, presumably, interaction between the two rock types could lead to sulphide saturation and the precipitation of Ni-Cu sulphides. The historical assay results of the spinifex-like ultramafic rocks in drillhole TROUT01-01 were not encouraging (up to 66 ppb Pt; Assessment File 74249); however, proximal electromagnetic conductors were not tested with diamond drilling and the basal contact of the 180 m thick ultramafic intercept was not reached. Glacial drift prospecting in Thompson has identified indicator minerals associated with Ni-Cu deposits (McLeneghan et al., 2012, 2013) and may prove a useful exploration technique here if the ultramafic rocks are not overlain by Phanerozoic cover.

Diamonds

Diamonds are principally mined from kimberlite, a rare rock type that is associated with the margins of ancient terranes (e.g., the Superior craton) and often identified through drift prospecting of glacial till deposits. Kimberlite indicator minerals occur in the till deposits of the Fox and Hayes rivers areas south and east of the examined drillholes (Fedikow et al., 2001; Nielsen and Fedikow, 2002; Keller, 2019; Gauthier et al., 2021; Gauthier and Hodder, 2022), suggesting that these diamondiferous rocks may occur in northeastern Manitoba. Exploration programs in the area, which included some of the examined drillholes (Assessment Files 74005, 94676, 74259), targeted potential source kimberlites; however, the source of the anomalous indicator minerals was not identified.

Acknowledgments

The author thanks W. Sharpe and N. Palacios Montenegro for enthusiastic and capable field assistance while core logging in Thompson; E. Ralph, C. Epp and P. Belanger for thorough logistical support and assistance at the Midland drillcore storage facility; and C. Böhm for a discussion on the geology of the area and helping navigate archival sample data. The companies that donated the examined drillcore to the Manitoba Geological Survey (Selco Exploration Company Ltd., Valerie Gold Resources Ltd., BHP Billiton Diamonds Inc. and Arctic Star Diamond Corporation)

are graciously thanked as well. Lastly, K. Reid and X.M. Yang are thanked for their constructive reviews and D. O'Hara is gratefully acknowledged for final editing and formatting of this report.

References

- Ansdell, K.M. 1993: U-Pb zircon constraints on the timing and provenance of fluvial sedimentary rocks in the Flin Flon and Athapapuskow basins, Flin Flon Domain, Trans-Hudson Orogen, Manitoba and Saskatchewan; *in* Radiogenic age and isotopic studies: report 7, Geological Survey of Canada, Paper 93-02, p. 49–57.
- Ansdell, K.M., Lucas, S.B., Connors, K.A. and Stern, R.A. 1995: Kisseynew metasedimentary gneiss belt, Trans-Hudson Orogen (Canada): back-arc origin and collisional inversion; Geology, v. 23, no. 11, p. 1039–1043.
- Bickford, M.E., Collerson, K.D., Lewry, J.F., Van Schmus, W.R. and Chiarenzelli, J.R. 1990: Proterozoic collisional tectonism in the Trans-Hudson orogen, Saskatchewan; Geology, v. 18, p. 14–18.
- Bleeker, W. 1990: New structural-metamorphic constraints on early Proterozoic oblique collision along the Thompson nickel belt, Manitoba, Canada; *in* The Early Proterozoic Trans-Hudson Orogen of North America, J.F. Lewry and M.R. Stauffer (ed.), Geological Association of Canada, Special Paper, v. 37, p. 57–73.
- Böhm, C.O., Hartlaub, R.P., Heaman, L., Cates, N., Guitreau, M., Bourdon, B., Roth, A.S.G., Mojzsis, S.J. and Blichert-Toft, J. 2019: The Assean Lake complex: ancient crust at the northwestern margin of the Superior Craton, Manitoba, Canada; chapter 6.2 *in* Earth's Oldest Rocks, M. Van Kranendonk, V.C. Bennet and J.E. Hoffmann (ed.), Developments in Precambrian Geology, v. 15, p. 751–774, URL https://doi.org/10.1016/S0166-2635(07)15096-9.
- Corkery, M.T. 1985: Geology of the lower Nelson River project area; Manitoba Energy and Mines, Geological Services, Geological Report 82-1, 66 p., plus 5 maps.
- Corrigan, D., Pehrsson, S., Wodicka, N. and de Kemp, E. 2009: The Paleoproterozoic Trans-Hudson Orogen: a prototype of modern accretionary processes; *in* Ancient Orogens and Modern Analogues, J.B. Murphy, J.D. Keppie and A.J. Hynes (ed.), Geological Society of London, Special Publications, v. 327, p. 457–479.
- David, J., Bailes, A.H. and Machado, N. 1996: Evolution of the Snow Lake portion of the Palaeoproterozoic Flin Flon and Kisseynew belts, Trans-Hudson Orogen, Manitoba, Canada; Precambrian Research, v. 80, no. 1–2, p. 107–124.
- Fedikow, M A.F., Nielsen, E., Conley, G.G. and Lenton, P.G. 2001: Operation Superior: kimberlite indicator mineral survey results (2000) for the northern half of the Knee Lake Greenstone Belt, Northern Superior Province, Manitoba (NTS 53M/1, 2, 3, 7 and 53L/15); Manitoba Industry, Trade and Mines, Geological Survey, Open File Report 2001-5, 57 p., URL https://www.manitoba.ca/iem/info/library/downloads/quaternary_and_surficial_geology.html [October 2025].
- Frohlinger, T.G. 1974: Geology of the Kettle Rapids—Long Spruce Rapids area, Manitoba Department of Mines, Resources and Environmental Management, Mineral Resources Division, Exploration and Geological Survey Branch, Summary of Geological Field Work, 1974, Geological Paper 2/74, p. 21–25, URL https://www.manitoba.ca/iem/info/libmin/GP2-74.pdf [September 2025].

- Gauthier, M.S. and Hodder, T.J. 2022: Kimberlite-indicator-mineral data derived from glacial sediments (till) in the western Fox River greenstone belt area, northeastern Manitoba (NTS 53M15, 16); Manitoba Natural Resources and Northern Development, Manitoba Geological Survey, Data Repository Item DRI2022010, Microsoft® Excel® file, URL https://manitoba.ca/iem/info/libmin/DRI2022010.xlsx [September 2025].
- Gauthier, M.S., Breckenbridge, A. and Hodder, T.J. 2021: Patterns of ice recession and ice stream activity for the MIS 2 Laurentide Ice Sheet in Manitoba, Canada; Boreas, v. 51, no. 2, p. 274–298.
- Gilbert, H.P., Syme, E.C. and Zwanzig, H.V. 1980: Geology of the metavolcanic and volcaniclastic metasedimentary rocks in the Lynn Lake area; Manitoba Energy and Mines, Mineral Resources Division, Geological Paper 80-1, 118 p., URL https://www.manitoba.ca/iem/info/libmin/GP80-1.zip [September 2025].
- Gordon, T.M. 1989: Thermal evolution of the Kisseynew sedimentary gneiss belt, Manitoba: metamorphism at an early Proterozoic accretionary margin; *in* Evolution of Metamorphic Belts, J.S. Daly, R.A. Cliff and B.W.D. Yardley (ed.), Geological Society, v. 43, p. 233–243.
- Gordon, T.M., Hunt, P.A., Bailes, A.H. and Syme, E.C. 1990: U-Pb ages from the Flin Flon and Kisseynew belts, Manitoba: chronology of crust formation at an Early Proterozoic accretionary margin; in The Early Proterozoic Trans-Hudson Orogen of North America, J.F. Lewry and M.R. Stauffer (ed.), Geological Association of Canada, Special Paper, v. 37, p. 177–199.
- Growdon, M. L. 2010: Crustal development and deformation of Laurentia during the Trans-Hudson and Alleghenian Orogenies; Ph.D. thesis, Indiana University at Bloomington, Indiana, 236 p.
- Hartlaub, R.P., Böhm, C.O., Heaman, L.M. and Simonetti, A. 2005: Northwestern Superior craton margin, Manitoba: an overview of Archean and Proterozoic episodes of crustal growth, erosion and orogenesis (parts of NTS 54D and 64A); *in* Report of Activities 2005, Manitoba Industry, Economic Development and Mines, Manitoba Geological Survey, p. 54-60, URL https://www.manitoba.ca/iem/geo/field/roa05pdfs/GS-07.pdf [September 2025].
- Haugh, I. and Elphick, S C. 1968: Kettle Rapids–Moose Lake area, Manitoba Mines and Natural Resources, Mines Branch, Geological Survey of Manitoba, Summary of Geological Fieldwork, 1968, Geological Paper 3/68, p. 29–37, URL https://www.manitoba.ca/iem/info/libmin/GP3-68.pdf [September 2025].
- Keller, G.R. 2019: Manitoba Kimberlite Indicator Mineral Database (version 3.2); Manitoba Growth, Enterprise and Trade, Manitoba Geological Survey, zipped Microsoft™ Access™ 2016 Database, URL https://www.gov.mb.ca/iem/geo/diamonds/MBKIMDB_32.zip [October 2025].
- Lawley, C.J.M., Yang, X.M., Selby, D., Davis, W., Zhang, S., Petts, D.C. and Jackson, S.E. 2020: Sedimentary basin controls on orogenic gold deposits: new constraints from U-Pb detrital zircon and Re-Os sulphide geochronology, Lynn Lake greenstone belt, Canada; Ore Geology Reviews, v. 126, p. 21.
- Lightfoot, P.C., Stewart, R., Gribbin, G. and Mooney, S.J. 2017: Relative contribution of magmatic and post-magmatic processes in the genesis of the Thompson Mine Ni-Co sulfide ores, Manitoba, Canada; Ore Geology Reviews, v. 83, p. 258–286.

- Macdonald, J. and Janssens, J. 2025: Whole-rock lithogeochemistry and assays for samples collected from archived drillcore east of Stephens Lake, northeastern Manitoba (parts of NTS 54C, D); Manitoba Business, Mining, Trade and Job Creation, Manitoba Geological Survey, Data Repository Item DRI2025024, file format Excel®, URL https://www.manitoba.ca/iem/info/libmin/DRI2025024.xlsx [October 2025].
- Machado, N., Zwanzig, H.V. and Parent, M. 1999: U-Pb ages of plutonism, sedimentation, and metamorphism of the Paleoproterozoic Kisseynew metasedimentary belt, Trans-Hudson Orogen (Manitoba, Canada); Canadian Journal of Earth Sciences, v. 36, no. 11, p. 1829–1842.
- Manitoba Geological Survey 2024: Bedrock geology of Manitoba; Manitoba Economic Development, Investment and Trade, Manitoba Geological Survey, Open File OF2024-4, scale 1:1 000 000.
- McLeneghan, M.B., Kjarsgaard, I.M., Averill, S.A., Layton-Matthews, D., Crabtree, D. and Matile, G. 2012: Indicator mineral signatures of magmatic Ni-Cu deposits, Thompson Nickel Belt, Manitoba: Part 1 bedrock data; Geological Survey of Canada, Open File 6766, 43 p.
- McLeneghan, M.B., Kjarsgaard, I.M., Averill, S.A., Layton-Matthews, D., Crabtree, D., Matile, G., McMartin, I. and Pyne, M. 2013: Indicator mineral signatures of magmatic Ni-Cu deposits, Thompson Nickel Belt, Manitoba: Part 2 till data; Geological Survey of Canada, Open File 7200, 148 p.
- Murphy, L.A. and Zwanzig, H.V. 2021: Geology of the Wuskwatim–Granville lakes corridor, Kisseynew domain, Manitoba (parts of NTS 63O, P, 64A–C); Manitoba Agriculture and Resource Development, Manitoba Geological Survey, Geoscientific Report GR2021-2, 105 p., URL https://www.manitoba.ca/iem/info/libmin/GR2021-2.zip [September 2025].
- Nielsen, E. and Fedikow, M.A.F. 2002: Kimberlite indicator-mineral survey, lower Hayes River; Manitoba Industry, Trade and Mines, Manitoba Geological Survey, Geoscientific Paper 2002-1, 39 p., URL https://www.manitoba.ca/iem/info/libmin/GP2002-1.zip [September 2025].
- Palin, R.M. and Dyck, B. 2021: Metamorphism of pelitic (Al-rich) rocks; in Encyclopedia of Geology, 2nd edition, A. Alderton and S.A. Elias (ed.), Elsevier, London, United Kingdom, p. 445–456, URL https://doi.org/10.1016/B978-0-08-102908-4.00081-3>.
- Pearce, J., Harris, N. and Tindle, A.G. 1984: Trace element discrimination diagrams for the tectonic interpretation of granitic rocks; Journal of Petrology, v. 25, p. 956–983.
- Rinne, M.L. 2018: Summary of key results and interpretations from the Fox River belt compilation project, northeastern Manitoba (parts of NTS 53M, N, O, 54B, C, D); Manitoba Growth, Enterprise and Trade, Manitoba Geological Survey, p. 25–36, URL https://www.manitoba.ca/iem/geo/field/roa18pdfs/GS2018-3.pdf [September 2025].
- Shervais, J.W. 1982: Ti-V plots and the petrogenesis of modern and ophiolitic lavas; Earth and Planetary Science Letters, v. 59, no. 1, p. 101–118.

- Stauffer, M.R. 1990: The Missi Formation: an Aphebian molasse deposit in the Reindeer Lake Zone of the Trans-Hudson Orogen, Canada; *in* The Early Proterozoic Trans-Hudson Orogen of North America, J.F. Lewry and M.R. Stauffer (ed.), Geological Association of Canada, Special Paper, v. 37, p. 121–141.
- Sun, S.-s. and McDonough, W.F. 1989: Chemical and isotopic systematics of oceanic basalts: implications for mantle composition and processes; *in* Magmatism in the Ocean Basins, A.D. Saunders and M.J. Norry (ed.), Geological Society, London, Special Publications, v. 42, p. 313–345, URL https://doi.org/10.1144/GSL.SP.1989.042.01.19>.
- Winchester, J.A. and Floyd, P.A. 1977: Geochemical discrimination of different magma series and their differentiation products using immobile elements; Chemical Geology, v. 20, p. 325–343.
- Yang, X.M. 2025: Geochemical data of 737 whole-rock samples from the Lynn Lake greenstone belt, northwestern Manitoba (parts of NTS 64C10–12, 14–16); Manitoba Business, Mining, Trade and Job Creation, Manitoba Geological Survey, Data Repository Item DRI2025004, Microsoft® Excel® file, URL https://www.manitoba.ca/iem/info/libmin/DRI2025004.xlsx [September 2025].
- Zwanzig, H.V. 1990: Kisseynew gneiss belt in Manitoba: stratigraphy, structure, and tectonic evolution; *in* The Early Proterozoic Trans-Hudson Orogen of North America, J.F. Lewry and M.R. Stauffer (ed.), Geological Association of Canada, Special Paper, v. 37, p. 95–120.

- Zwanzig, H.V. 1999: Updated trace element geochemistry of ca. 1.9 Ga metavolcanic rocks in the Paleoproterozoic Lynn Lake belt; Manitoba Industry, Trade and Mines, Geological Services, Manitoba Geological Survey, Open File Report 99-13, URL https://www.manitoba.ca/iem/info/libmin/OF99-13.zip [October 2025]
- Zwanzig, H.V. and Bailes, A.H. 2010: Geology and geochemical evolution of the northern Flin Flon and southern Kisseynew domains, Kississing-File lakes area, Manitoba (parts of NTS 63K, N); Manitoba Innovation, Energy and Mines, Manitoba Geological Survey, Geoscientific Report 2010-1, 135 p., URL https://www.manitoba.ca/iem/info/libmin/GR2010-1.zip [September 2025].
- Zwanzig, H.V. and Böhm, C.O. 2004: Northern extension of the Thompson Nickel Belt, Manitoba (NTS 64A3 and 4); *in* Report of Activities 2004, Manitoba Industry, Economic Development and Mines, Manitoba Geological Survey, p. 115–119, URL https://www.manitoba.ca/iem/geo/field/roa04pdfs/GS-10.pdf [September 2025].
- Zwanzig, H.V., Macek, J.J. and McGregor, C.R. 2007: Lithostratigraphy and geochemistry of the high-grade metasedimentary rocks in the Thompson nickel belt and adjacent Kisseynew Domain, Manitoba: implications for nickel exploration; Economic Geology, v. 102, no. 7, p. 1197–1216, URL https://doi.org/10.2113/gsecongeo.102.7.1197>.